Bull. Chem. Soc. Ethiop. **2022**, 36(2), 433-450. ISSN 1011-3924
© 2022 Chemical Society of Ethiopia and The Authors Printed in Ethiopia
DOI: https://dx.doi.org/10.4314/bcse.v36i2.16 Online ISSN 1726-801X

# NOVEL AND HIGH EFFICIENT CYCLOADDITION OF $CO_2$ WITH EPOXIDES TO CYCLIC CARBONATES OVER REUSABLE MESOPOROUS KIT-6 SUPPORTED IMIDAZOLIUM LACTATE CATALYST

Yang Liu[1] and Yu Lin Hu[1,2*]

[1]College of Materials and Chemical Engineering, Key laboratory of inorganic nonmetallic crystalline and energy conversion materials, China Three Gorges University, Yichang 443002, China
[2]Hubei Three Gorges Laboratory, Yichang 443007, China

(Received March 1, 2022; Revised March 31, 2022; Accepted March 31, 2022)

**ABSTRACT**. A series of mesoporous KIT-6 supported ionic liquids were prepared and tested as effective and practical catalysts for the synthesis of cyclic carbonates by the cycloaddition of $CO_2$ with epoxides. The effects of type of catalysts, catalyst amount, $CO_2$ pressure, reaction temperature and catalyst stability have also been investigated in detail, the catalyst KIT-6@ILCH$_3$CH(OH)COO(0.6) exhibited excellent activity in good to excellent yields, may be attributed to the synergetic effect between hydroxyl groups and lactate anion of the ionic liquid. In addition, the supported catalyst can be easily recovered and reused for six times still with satisfactory catalytic activity. Moreover, a general synergetic catalytic mechanism for the reaction was proposed. This work introduces a new and highly efficient pathway to explore the supported ionic liquids for the chemical fixation of carbon dioxide.

**KEY WORDS**: Mesoporous KIT-6, Ionic liquid, High efficient, Carbon dioxide, Cyclic carbonates, Recyclable catalyst

## INTRODUCTION

Utilization of carbon dioxide ($CO_2$) as a carbon building block to produce the valuable chemicals has attracted considerable attention due to its prominent feature of abundance, nontoxicity, non-expensive, and recyclability [1-3]. Among possible processes, the selective coupling reaction of $CO_2$ with epoxides is promising due to both the view of 100% atomic economy and the wide applications of cyclic carbonates products, which have widely been employed as intermediates to produce pharmaceuticals, polymers and fine chemicals [4-6]. Thus, the chemical fixation of $CO_2$ with epoxides for the synthesis of cyclic carbonates has attracted an immense interest, and a large number of catalysts have been reported for the cycloaddition such as hollow marigold $CuCo_2O_4$ [7], organocatalysts [8-10], metal complexes [11-13], MMFR250 [14], MOFs [15-17], CoPc/$TiO_2$ Hybrid [18], ChI-HBD [19], and others [20-26]. Nevertheless, most of these protocols still suffered from disadvantages such as the stoichiometric use of catalysts, harsh reaction conditions, tedious isolation techniques, and catalyst recycle problems. In this regard, the development novel, sustainable and efficient catalytic systems for the synthesis of cyclic carbonates from epoxides and $CO_2$ are highly recommendable.

Ionic liquids (ILs), as a charming functional material, have found various industrial applications in synthesis and catalysis due to their negligible vapour pressure, thermal and chemical stability, non-flammable, nonvolatile and strong structural design prospects [27-37]. Through the functional design of anions and cations of ionic liquids, the use of ILs as catalysts in the efficient synthesis of cyclic carbonates have been developed [38-42]. However, the isolation of pure ILs from products and reusability has been the major issue in these processes in view of eco-sustainability. Therefore, the immobilization of these functionalized ILs over different solid supports to explore heterogeneous supported ILs has made the process easier through their easy handling, thermal stability, facile isolation and reusability [43-46]. Among these solid supports,

---

*Corresponding author. E-mail: huyulin1982@163.com

mesoporous silica materials offer significant advantages of large surface area, highly ordered structure, thermal and chemical stabilities. These materials can be used as a platform for the loading and dispersion of ILs active components, thereby increasing their catalytic activities and have been widely utilized as supports in the case of heterogeneous catalysis [47-50]. In this work, we wish to report the design and synthesis of a type of mesoporous KIT-6 supported imidazolium hydrogen carbonate functionalized ionic liquids. These supported ionic liquids with different ionic liquid concentration have been employed as recyclable and high-efficient heterogeneous catalysts for the product of cyclic carbonates by the cycloaddition of $CO_2$ with epoxides under mild conditions (Scheme 1). Furthermore, the recycling performance of catalyst and possible catalytic mechanism were explored.

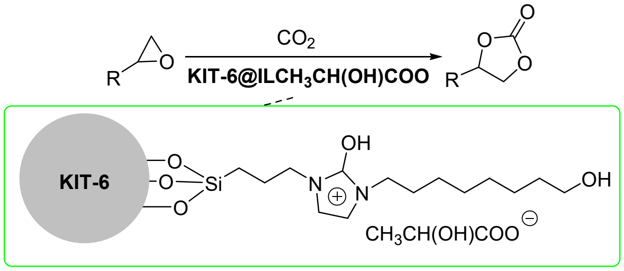

Scheme 1. Catalytic cycloaddition of $CO_2$ with epoxides into cyclic carbonates.

## EXPERIMENTAL

### *Materials and apparatus*

Pluronic 123 ($EO_{20}PO_{70}EO_{20}$) was purchased from Sigma-Aldrich, and other reagents were of analytical grade and used without any further purification. Scanning electron microscopy (SEM) and energy dispersive X-ray spectroscopy (EDX) were carried out on a JSM-7500F electron microscope. FT-IR spectra were recorded on a PE Fourier Transform spectrometer. Powder X-ray diffraction (XRD) data were obtained using Ultima IV diffractometer. The thermogravimetric analysis (TGA) was carried out on a NETZSCH STA 449 F5 at a heating rate of 10 °C $min^{-1}$ under nitrogen. UV-Vis spectra were recorded on a Shimadzu UV-2450 spectrophotometer. $N_2$ adsorption–desorption isotherms were recorded using a BELSORP-max instrument and pore size distribution curves were calculated from the analysis of desorption branch of the isotherm by the BJH (Barrett–Joyner–Halenda). $^1H$ NMR spectra were recorded on a Bruker 400 MHz spectrometer. Elemental analysis was recorded on a Vario Micro cube Elemental Analyzer. GC analysis were carried out by Agilent 7890 with flame ionization detector.

### *Synthesis of KIT-6 supported ILs*

KIT-6 was synthesized as described in literatures [48, 49]. The supported ILs were synthesized according to literatures (Scheme 2) [43-46]. A typical procedure was as follows: sodium ethoxide (0.4 mol), ethanol (200 mL) and 2-hydroxyimidazole (0.4 mol) were stirred at 70 ºC for 8 h to give **1**. Next, (3-chloropropyl) triethoxysilane (0.4 mol) was added, and the reaction mixture was refluxed for 24 h. After evaporating the solvent, the mixture was washed with ethyl acetate and dried under vacuum to give **2**. Subsequently, 8-chlorooctan-1-ol (0.2 mol), and **2** (0.2 mol), and toluene (200 mL) were stirred at 90 ºC under nitrogen for 24 h, thereafter, the solvent was isolated and dried to give **3**. Then, **3** (0.1 mol), sodium lactate (0.1 mol), ethanol (70 mL) were stirred at 60 °C for 24 h, then the solvent was evaporated, the obtained residue was washed with water and dried under vacuum to give ionic liquid **4** $ILCH_3CH(OH)COO$. Finally, KIT-6 (1.0 g) and **4** (x g) were added into a solution of dry toluene (100 mL), and the mixture was stirred and refluxed for 24 h under nitrogen. Then the resulting solid was filtered, cleansed twice with diethyl ether and dried under vacuum for obtaining the supported IL KIT-6@ILCH$_3$CH(OH)COO(x).

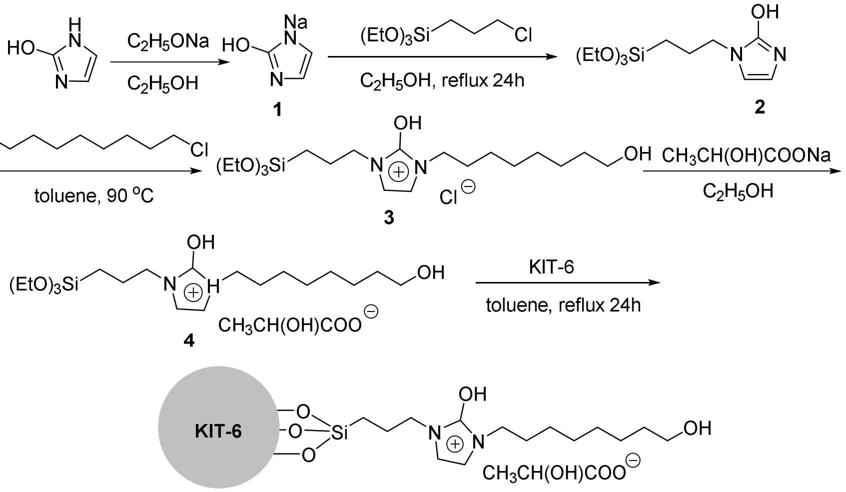

Scheme 2. Schematic diagram of supported ionic liquids fabrications.

*Catalytic synthesis of cyclic carbonates*

In a typical procedure, epoxide (0.01 mol), KIT-6@ILCH$_3$CH(OH)COO(0.6) (0.15 g) were added into a 50 mL stainless-steel autoclave with the stirrer, and then $CO_2$ was introduced into the autoclave and kept for 0.7 MPa pressure after the air evacuated. The autoclave was heated to 90 °C for a desired time under vigorous stirring. Upon the completion of the reaction, the remaining $CO_2$ was released slowly. Meanwhile, the reactor was cooled to room temperature and the product was obtained by filtration and separation. The product was quantitatively analyzed by GC. Fresh substrates were then recharged to the recovered catalyst and then recycled under identical reaction conditions. All target products are known, thus they were recognized by comparison with those of standard compounds or by $^1$H NMR and elemental analysis. Spectroscopic data for products is as follows.

Propylene carbonate (Table 2, entry 1): $^1$H NMR (400 MHz, $CDCl_3$, $\delta$ ppm) 1.47 (dd, $CH_3$, 3H), 3.98 (t, CH, 1H), 4.51 (t, CH, 1H), 4.83 (m, CH, 1H); elemental analysis for $C_4H_6O_3$: C, 47.02; H, 5.90; O, 46.97. Found C, 47.06; H, 5.92; O, 47.01.

1,3-Dioxolan-2-one (Table 2, entry 2): $^1$H NMR: $\delta$ 4.53 (s, $CH_2CH_2$, 4H). Anal. calcd. for $C_3H_4O_3$: C, 40.88; H, 4.56; O, 54.48. Found: C, 40.92; H, 4.58; O, 54.50.

4,4-Dimethyl-1,3-dioxolan-2-one (Table 2, entry 3): $^1$H NMR: $\delta$ 1.45 (s, $2CH_3$, 6H), 4.23 (s, $CH_2$, 2H). Anal. Calcd. for $C_5H_8O_3$: C, 51.69; H, 6.93; O, 41.31. Found: C, 51.72; H, 6.94; O, 41.34.

(Chloromethyl)ethylene carbonate (Table 2, entry 4): $^1$H NMR (400 MHz, $CDCl_3$, $\delta$ ppm) 3.75 (dd, $CH_2$, 2H), 4.34 (t, $CH_2$, 1H), 4.57 (t, $CH_2$, 1H), 4.93 (m, CH, 1H); elemental analysis for $C_4H_5ClO_3$: C, 35.16; Cl, 25.92; O, 35.11. Found C, 35.19; Cl, 25.96; O, 35.15.

Hexahydrobenzo[d][1,3]dioxol-2-one (Table 2, entry 5): $^1$H NMR (400 MHz, $CDCl_3$, $\delta$ ppm) 1.35-1.46 (m, $CH_2CH_2$, 4H), 1.74-1.82 (m, $2CH_2$, 4H), 5.24 (t, 2CH, 2H); elemental analysis for $C_7H_{10}O_3$: C, 59.12; H, 7.05; O, 33.73. Found C, 59.15; H, 7.09; O, 33.76.

Styrene carbonate (Table 2, entry 6): $^1$H NMR (400 MHz, $CDCl_3$, δ ppm) 4.32 (t, $CH_2$, 1H), 4.73 (t, $CH_2$, 1H), 5.67 (t, $CH_2$, 1H), 7.26-7.39 (m, Ar-H, 5H); elemental analysis for $C_9H_8O_3$: C, 65.82; H, 4.87; O, 29.21. Found C, 65.85; H, 4.91; O, 29.24.

## RESULTS AND DISCUSSION

XRD patterns of all samples are showed in Figure 1. Compared to the XRD pattern of pure KIT-6, the spectra of pure KIT-6 and supported ILs are almost the same, only one broad peak appears at about $2\theta = 23.4°$, which is the characteristic beta zeolite structure of KIT-6 [48-50]. No typical peaks corresponding to ionic liquids were observed, suggested that the ionic liquid species were well-dispersed on the parent support framework. The surface morphology and elemental composition of the supported ILs catalysts are characterized by SEM and EDX techniques. As can be seen from the SEM image (Figure 2), the KIT-6 exhibited characteristic rock-like morphology. After the immobilization of ionic liquid on the KIT-6 support, the typical aggregated small spherical particles can be seen in the beta zeolite, and the particles which are aggregated into big block constitute the Beta seed. The SEM images of KIT-6 and KIT-6 supported ionic liquids indicated that both of them have irregular particle morphologies, which are almost identical to the literature [48-50]. The EDX images of the supported ILs are exhibited in Figure 3, in which the corresponding elemental signals were distributed homogeneously and consistently, indicating the successful formation of the supported ILs species as well.

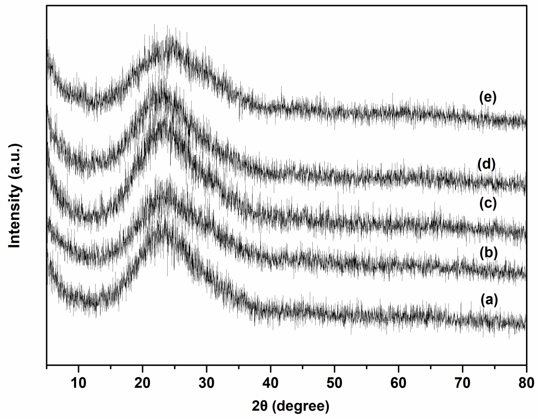

Figure 1. XRD patterns of KIT-6@IL$CH_3CH(OH)COO$(0.2) (a), KIT-6@IL$CH_3CH(OH)COO$(0.4) (b), KIT-6@IL$CH_3CH(OH)COO$(0.6) (c), KIT-6@IL$CH_3CH(OH)COO$(0.8) (d), and KIT-6 (e).

Similar results are obtained by UV–Vis characterization (Figure 4), the intensity of diffraction peak at around 223 nm is attributed to Si-O species of KIT-6 [48-50]. Obviously, after immobilization of ionic liquids, no significant peaks attributed to the ionic liquids particles are found in the UV–Vis patterns, which may be owing to the well-dispersed ionic liquids particles encapsulated in mesoporous channels of the KIT-6 support. Moreover, FT-IR spectra of the supported ionic liquids are shown in Figure 5. The peaks in the absorption band from 3620 to 3340 cm$^{-1}$ suggested the existence of hydroxyl stretching vibration. The peak at around 1732 cm$^{-1}$ is ascribed to the presence of C=O, and the peak at around 1093 cm$^{-1}$ is ascribed to the presence of Si–O–Si. The peak observed at around 748 cm$^{-1}$ is ascribed to the $CH_2$ chain flexural vibration of lactate. The vibrations of N=N and C–N bonds of imidazole generated the observed peaks at around 1613 cm$^{-1}$ and 1541 cm$^{-1}$, respectively [27-29, 43-46]. In addition, BET analysis of KIT-6@IL$CH_3CH(OH)COO$(0.6) is presented Table 1. As can be seen in the table, there is a huge reduction in the surface area, pore volume, and the pore diameter of KIT-6@IL$CH_3CH(OH)COO$(0.6) after the immobilization of ionic liquid on the KIT-6 support, thereby confirming that the pores are filled with ionic liquids nanoparticles. It should be noted that both KIT-6@IL$CH_3CH(OH)COO$(0.6) and KIT-6 showed a type IV adsorption isotherm with a sharp condensation step and hysteresis loop, which is indicative of materials with a well-ordered mesoporous structure (Figure 6) [48, 49].

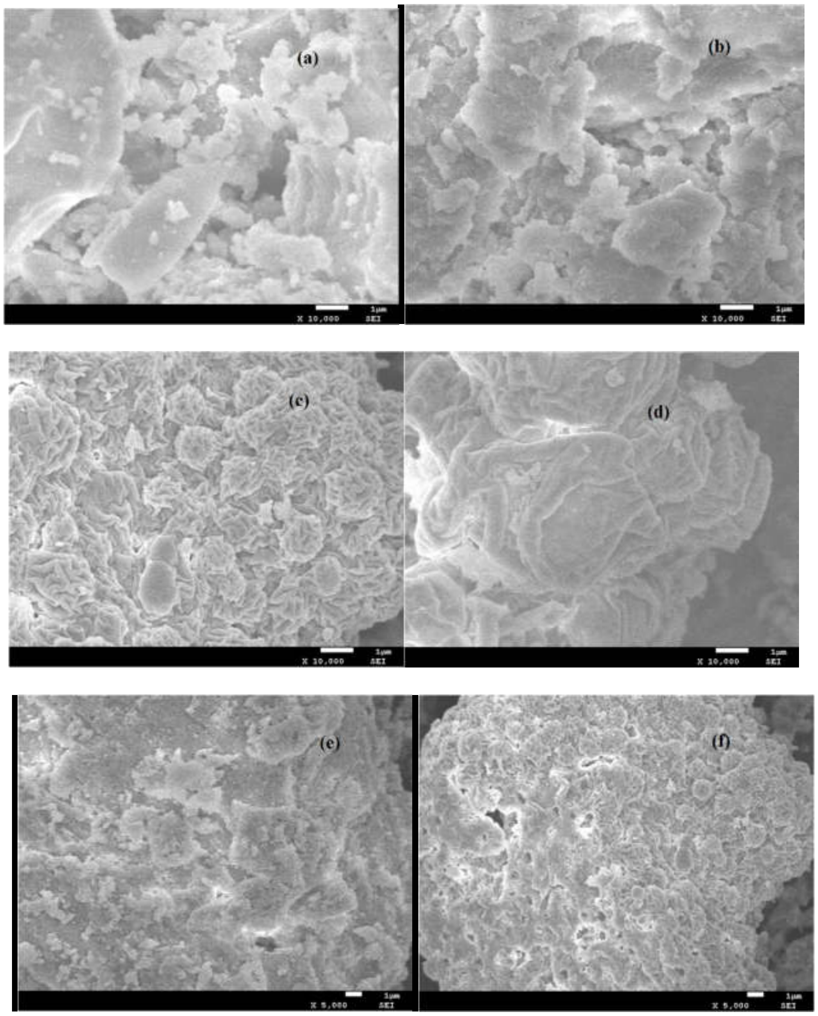

Figure 2. SEM images of KIT-6@IL$CH_3CH(OH)COO$(0.2) (a), KIT-6@IL$CH_3CH(OH)COO$(0.4) (b), KIT-6@IL$CH_3CH(OH)COO$(0.6) (c), KIT-6@IL$CH_3CH(OH)COO$(0.8) (d), KIT-6 (e), and six times recovered KIT-6@IL$CH_3CH(OH)COO$(0.6) (f).

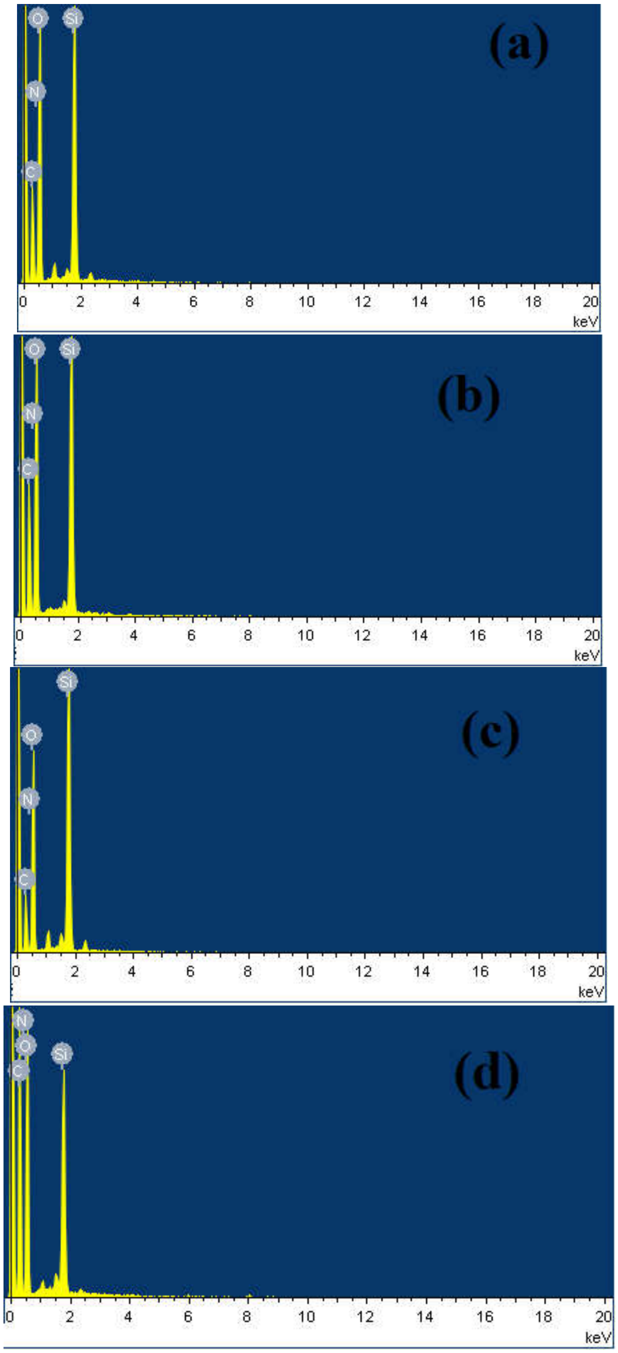
(a)
O
Si
N
C
0
2
4
6
8
10
12
14
16
18
20
keV
(b)
O
Si
N
C
(c)
Si
O
N
C
(d)
N
O
C
Si

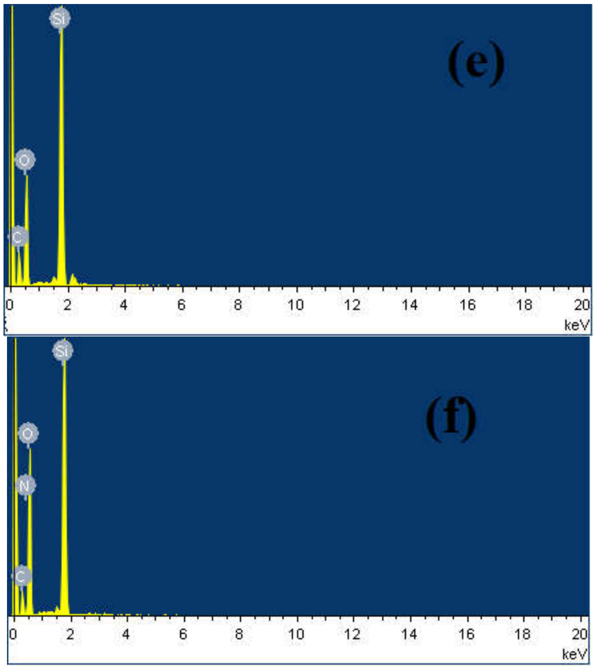

Figure 3. EDX images of KIT-6@ILCH$_3$CH(OH)COO(0.2) (a), KIT-6@ILCH$_3$CH(OH)COO(0.4) (b), KIT-6@ILCH$_3$CH(OH)COO(0.6) (c), KIT-6@ILCH$_3$CH(OH)COO(0.8) (d), KIT-6 (e), and six times recovered KIT-6@ILCH$_3$CH(OH)COO(0.6) (f).

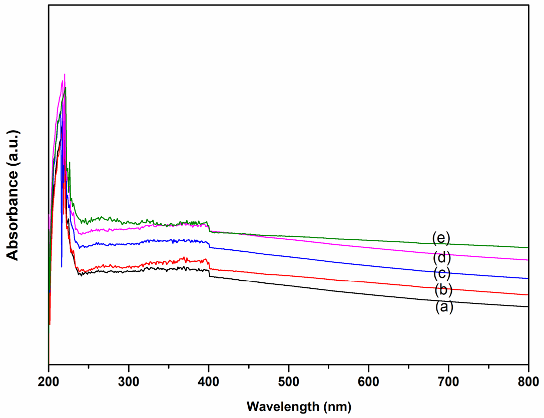

Figure 4. UV–Vis spectras of KIT-6@ILCH$_3$CH(OH)COO(0.2) (a), KIT-6@ILCH$_3$CH(OH)COO(0.4) (b), KIT-6@ILCH$_3$CH(OH)COO(0.6) (c), KIT-6@ILCH$_3$CH(OH)COO(0.8) (d), and KIT-6 (e).

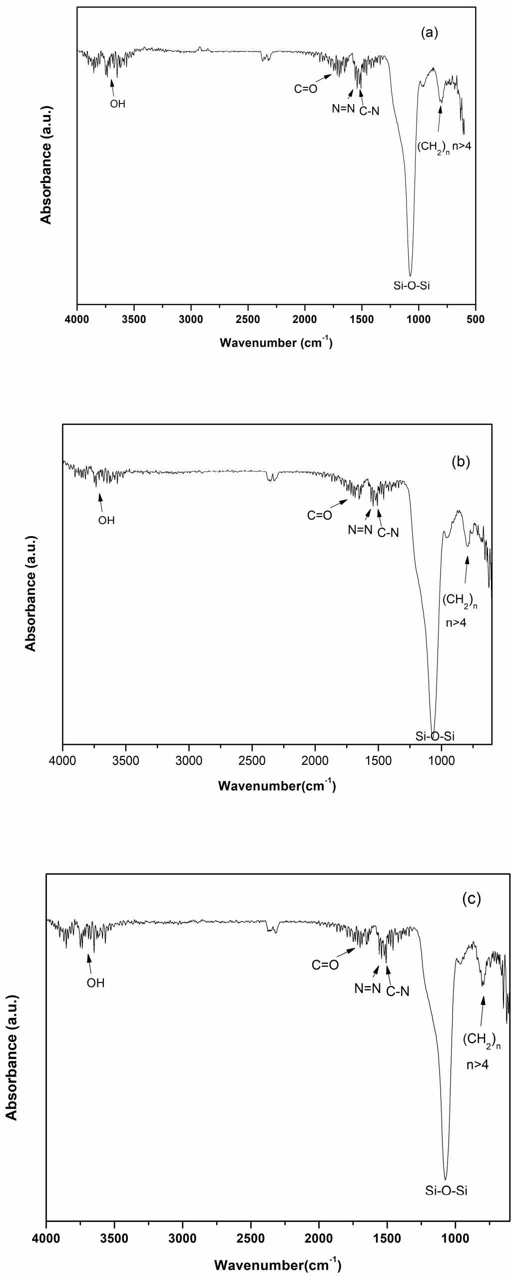
(a)
OH
C=O
N=N
C-N
$(CH_2)_n$ n>4
Si-O-Si
Absorbance (a.u.)
Wavenumber (cm$^{-1}$)
4000
3500
3000
2500
2000
1500
1000
500
(b)
OH
C=O
N=N
C-N
$(CH_2)_n$
n>4
Si-O-Si
Absorbance (a.u.)
Wavenumber(cm$^{-1}$)
4000
3500
3000
2500
2000
1500
1000
(c)
OH
C=O
N=N
C-N
$(CH_2)_n$
n>4
Si-O-Si
Absorbance (a.u.)
Wavenumber(cm$^{-1}$)
4000
3500
3000
2500
2000
1500
1000

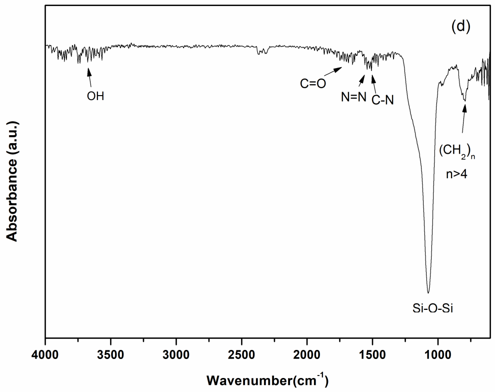

Figure 5. FT-IR spectras of KIT-6@$ILCH_3CH(OH)COO$(0.2) (a), KIT-6@$ILCH_3CH(OH)COO$(0.4) (b), KIT-6@$ILCH_3CH(OH)COO$(0.6) (c), KIT-6@$ILCH_3CH(OH)COO$(0.8) (d).

Table 1. BET surface area and pore volume of KIT-6@$ILCH_3CH(OH)COO$(0.6) and KIT-6.

| Sample | $A_{BET}$ ($m^2/g$)[a] | $V_p$ ($cm^3/g$)[b] | $d_{pBJH}$ (nm)[c] |
|---|---|---|---|
| KIT-6 | 664.86 | 1.0965 | 8.1282 |
| KIT-6@$ILCH_3CH(OH)COO$(0.6) | 379.24 | 0.7319 | 6.8191 |

[a]Specific surface area obtained using a Brunauer-Emmett-Teller (BET) plot. [b]Specific pore volume. [c]Pore diameter obtained using the Barrett-Joyner-Halenda method.

Initially, the catalytic synthesis of propylene carbonate by the cycloaddition of propylene oxide with $CO_2$ was chose as the model reaction for the optimization of reaction conditions (Table 2). It can be observed that the bulk ionic liquid $ILCH_3CH(OH)COO$ or mesoporous support KIT-6 as catalyst has low yields of propylene carbonate, which suggested that bulk $ILCH_3CH(OH)COO$ and mesoporous support KIT-6 were not effective catalysts for the cycloaddition (Table 2, entries 5 and 6). In addition, when catalyst was inexistence, no product was found even after longer reaction time of 24 h (Table 2, entry 7). In contrast, the as-prepared supported ionic liquids with different ionic liquid concentration could promote the catalytic process significantly, and drastic increase in the product yields and selectivities were achieved within shorter reaction times of 3~6 h (Table 2, entries 1-4). It was found that KIT-6@$ILCH_3CH(OH)COO$(0.6) demonstrated the highest catalytic performance with 97% yield and 99.6% selectivity (Table 2, entry 3). To further improve the activity, the effect of dosage of best catalyst KIT-6@$ILCH_3CH(OH)COO$(0.6) was studied. As shown in the table, the product yield is sharply increased from 53% to 92% when the catalyst amount is increased from 0.02 g to 0.1 g (Table 2, entries 8-10). After a steady growth, the product yield reaches 97% with the 0.15 g catalyst dosage (Table 2, entry 3). However, the catalyst dosage was further increased to 0.2 g, no obvious enhancement of product yield and selectivity were observed (Table 2, entry 11). Therefore, the suitable ionic liquid concentration and catalyst dosage are the more important to achieve the desired goal.

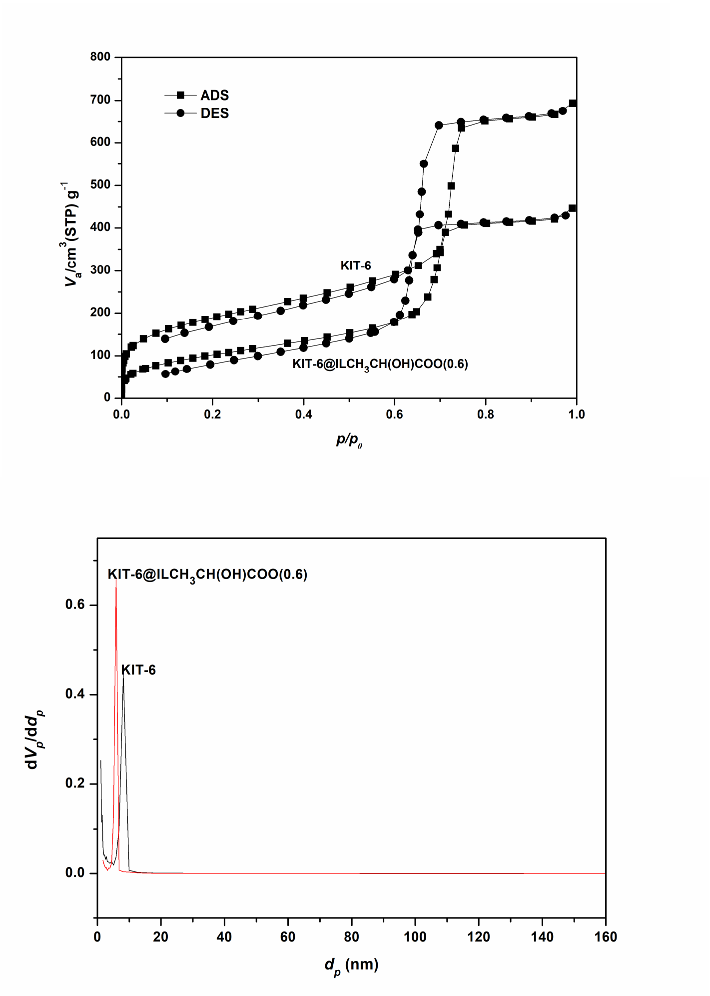

Figure 6. Nitrogen adsorption isotherms and size distribution of KIT-6@ILCH$_3$CH(OH)COO(0.6) and KIT-6.

Having found the best catalyst for the catalytic synthesis of propylene carbonate, reaction parameters such as $CO_2$ pressure and reaction temperature were optimized. The cycloaddition was remarkably influenced by the $CO_2$ pressure. As shown in Figure 7a, the product yield and selectivity was increased with an increase in the $CO_2$ pressure from 0.1 MPa to 0.7 MPa, however, no appreciable increase in the product yield and selectivity was noticed above this pressure. It was because $CO_2$ was compressed and present in the liquid phase at pressures below 0.7 MPa, thus resulting in improve the product yield and selectivity. At pressures higher than 0.7 MPa, propylene oxide was present in the gaseous form, which decrease the concentration and retard the interaction with KIT-6@ILCH$_3$CH(OH)COO(0.6), therefore no further improvement in the product yield and selectivity. It clearly illustrated that 0.7 MPa is the optimum $CO_2$ pressure. Figure 7b showed that the reaction temperature exhibited remarkable influence on the cycloaddition. The product yield and selectivity was increased with an increase in the reaction temperature from 40 °C to 90 °C, however, a slight decrease in the product yield and selectivity was observed above 90 °C. It was because both isomerization and ring opening of propylene oxide side reactions were observed at temperature higher than 90 °C (GC analysis). Therefore, 90 °C was selected as the optimum reaction temperature.

Table 2. Screening of catalysts for the cycloaddition of propylene oxide with $CO_2$ to produce propylene carbonate.[a]

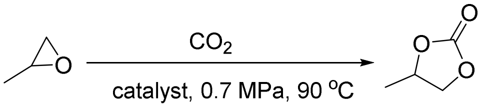

| Entry | Catalyst | Catalyst (g) | Time (h) | Yield (%)[b] | Selectivity (%)[c] |
|---|---|---|---|---|---|
| 1 | KIT-6@ILCH$_3$CH(OH)COO(0.2) | 0.15 | 6 | 81 | 98.6 |
| 2 | KIT-6@ILCH$_3$CH(OH)COO(0.4) | 0.15 | 4 | 90 | 99.1 |
| 3 | KIT-6@ILCH$_3$CH(OH)COO(0.6) | 0.15 | 3 | 97 | 99.6 |
| 4 | KIT-6@ILCH$_3$CH(OH)COO(0.8) | 0.15 | 3 | 93 | 98.8 |
| 5 | ILCH$_3$CH(OH)COO | 0.2 | 8 | 78 | 95.4 |
| 6 | KIT-6 | 0.2 | 12 | 26 | 89.2 |
| 7 | - | - | 24 | 0 | 0 |
| 8 | KIT-6@ILCH$_3$CH(OH)COO(0.6) | 0.02 | 6 | 53 | 98.5 |
| 9 | KIT-6@ILCH$_3$CH(OH)COO(0.6) | 0.05 | 5 | 74 | 98.9 |
| 10 | KIT-6@ILCH$_3$CH(OH)COO(0.6) | 0.1 | 4 | 92 | 99.3 |
| 11 | KIT-6@ILCH$_3$CH(OH)COO(0.6) | 0.2 | 3 | 96 | 99.0 |

[a]Reaction conditions: propylene oxide (0.01 mol), $CO_2$ pressure (0.7 MPa), 90 °C. [b]Isolated yield. [c]Calculated by GC analysis.

The important indicator to measure the pros and cons for the design of catalyst is the stability evaluation of the catalyst KIT-6@ILCH$_3$CH(OH)COO(0.6). As shown in Figure 7c, recycling catalytic experiments over KIT-6@ILCH$_3$CH(OH)COO(0.6) were carried out using the model reaction under the optimized conditions. The catalyst KIT-6@ILCH$_3$CH(OH)COO(0.6) was easily isolated by filtration and can be used directly for consecutive runs. Remarkably, KIT-6@ILCH$_3$CH(OH)COO(0.6) possessed a good reusability and maintained high catalytic performance at least six times without considerable reduction in catalytic activity. The product yield in the six run was 90%, showing merely a 7% decrease in performance compared to the fresh catalyst. The stability of KIT-6@ILCH$_3$CH(OH)COO(0.6) was also confirmed by the thermal gravimetric analysis (Figure 7d). The first step of weight loss (3.76%) below 200 °C was related to the removal of adsorbed water and other volatile solvent residues, whereas the main weight loss (12.32%) from 200 to 600 °C in the second step was corresponded to degradation of the organic moieties of ionic liquid. These observations demonstrated that the catalyst KIT-6@ILCH$_3$CH(OH)COO(0.6) was thermally stable below 200 °C, which was beneficial for the recycling catalytic experiments. The recovered catalyst after six cycles has no obvious change in morphology (Figure 2f). The EDX analysis of KIT-6@ILCH$_3$CH(OH)COO(0.6) after six cycles showed the existence of expected elemental signals (Figure 3f), which indicated that the catalyst remain stable after six cycles. The recovered catalyst after six times has no obvious change in crystalline structure, referring to the XRD pattern in comparison with the fresh catalyst (Figure 7e). Hence, the excellent stability and reusability of KIT-6@ILCH$_3$CH(OH)COO(0.6) made it possible for commercial applications.

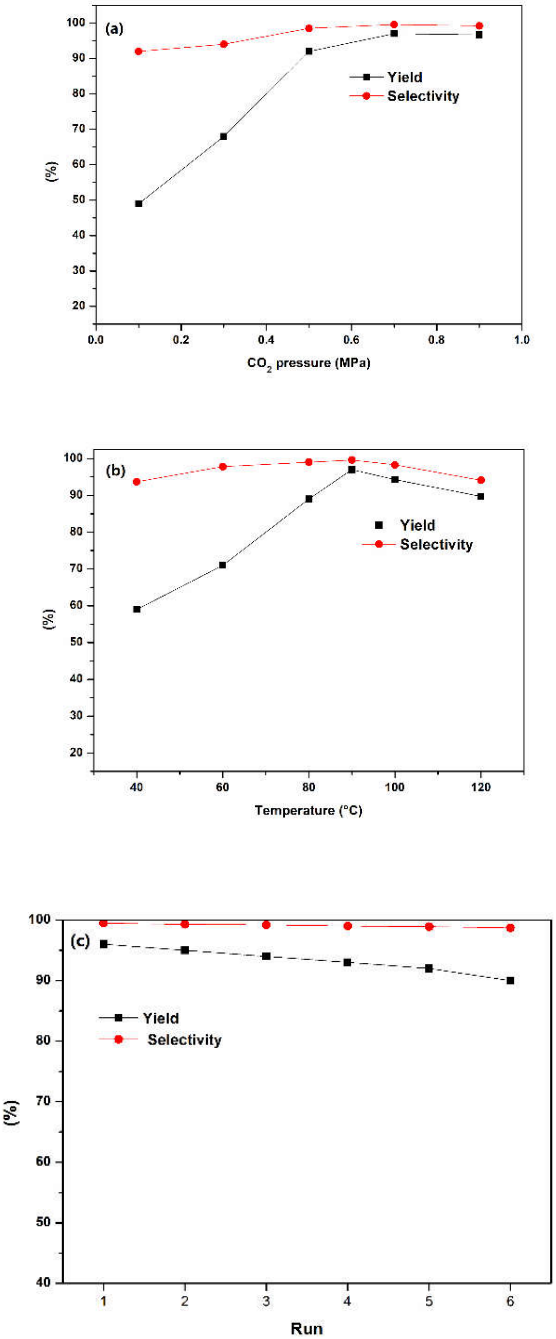
(a)
Yield
Selectivity
(%)
100
90
80
70
60
50
40
30
20
0.0
0.2
0.4
0.6
0.8
1.0
$CO_2$ pressure (MPa)
(b)
Yield
Selectivity
(%)
100
90
80
70
60
50
40
30
20
40
60
80
100
120
Temperature (°C)
(c)
Yield
Selectivity
(%)
100
90
80
70
60
50
40
1
2
3
4
5
6
Run

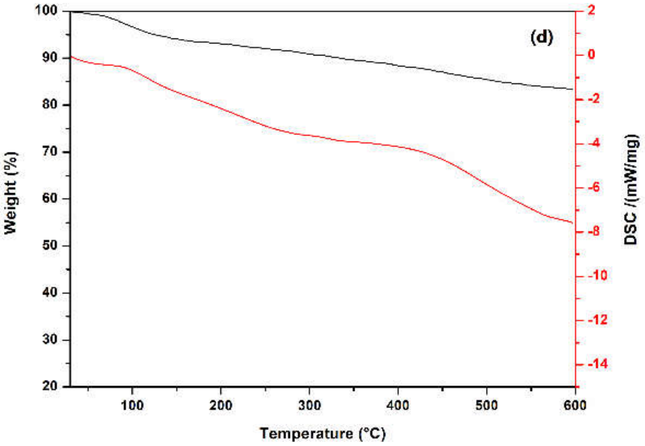

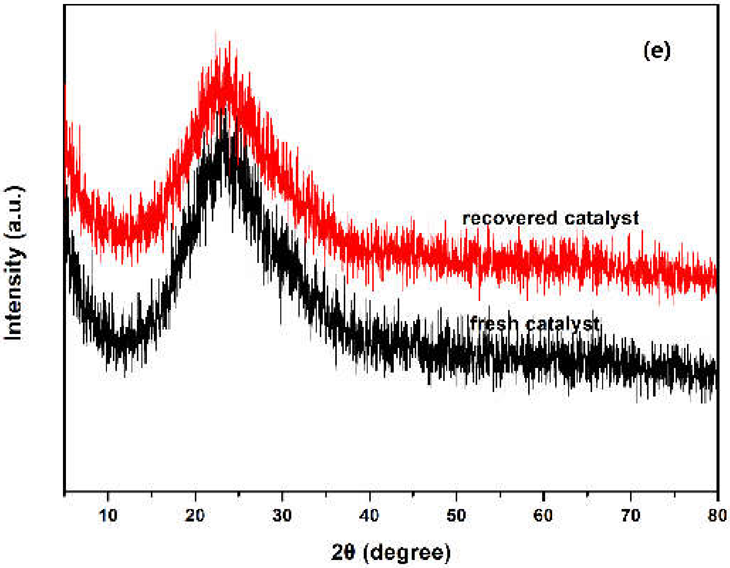

Figure 7.(a) Influence of $CO_2$ pressure in the cycloaddition (propylene oxide 0.01 mol, KIT-6@ILCH$_3$CH(OH)COO(0.6) 0.15 g, 90 °C, 3 h), (b) influence of reaction temperature in the cycloaddition (propylene oxide 0.01 mol, $CO_2$ pressure 0.7 MPa, KIT-6@ILCH$_3$CH(OH)COO(0.6) 0.15 g, 3 h), (c) recyclability chart of reused KIT-6@ILCH$_3$CH(OH)COO(0.6), (d) thermogravimetric analysis of KIT-6@ILCH$_3$CH(OH)COO(0.6), (e) XRD patterns of the fresh and recovered KIT-6@ILCH$_3$CH(OH)COO(0.6).

After having the optimized conditions in hand, we explored the generality of our developed protocol by employing other epoxides and the corresponding catalytic activities were showed in Table 3. The corresponding cyclic carbonates were obtained in good to high yields with excellent selectivities (>99%) within 5 h. When the substituted group is chloromethyl, the yield of (chloromethyl)ethylene carbonate is the highest due to the substitution of active methylene (Table 3, entry 4). The yield of hexahydrobenzo[d][1,3]dioxol-2-one is the lowest because of the high steric hindrance of cyclohexene oxide (Table 3, entry 5).

Table 3. Cycloaddition of $CO_2$ and different epoxides catalyzed by KIT-6@ILCH$_3$CH(OH)COO(0.6).[a]

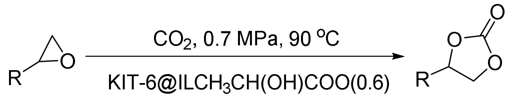

| Entry | Epoxide | Product | Time (h) | Yield (%)[b] | Selectivity (%)[c] |
|---|---|---|---|---|---|
| 1 | 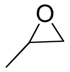 | 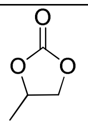 | 3 | 97 | 99.6 |
| 2 |  | 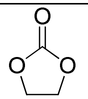 | 3 | 98 | 99.2 |
| 3 |  | 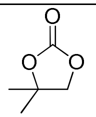 | 3 | 90 | 99.1 |
| 4 | 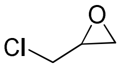 | 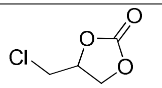 | 2 | 99 | 99.3 |
| 5 | 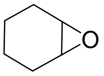 | 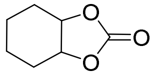 | 5 | 87 | 99.1 |
| 6 | 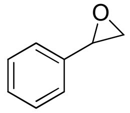 | 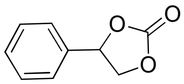 | 3 | 93 | 99.2 |

[a]Reaction conditions: epoxide (0.01 mol), KIT-6@ILCH$_3$CH(OH)COO(0.6) (0.15 g), $CO_2$ (0.7 MPa), 90 °C. [b]Isolated yield. [c]Calculated by GC analysis.

Based on the above results and relevant literatures [18-22], a possible catalytic mechanism is proposed for the cycloaddition of $CO_2$ with epoxides (Scheme 3). The first step involves the activation of epoxide by the O atom coordination with hydroxyl sites of the catalyst KIT-6@ILCH$_3$CH(OH)COO(0.6) for the formation of intermediate **i**. At the same time, the multifunctional catalyst helps to activate $CO_2$ for the formation of the carbonate species. Subsequently, the intermediate **i** adds to the less sterically hindered C atom of epoxide by nucleophilic attack to give the intermediate **ii**, followed by the nucleophilic interaction to give the intermediate **iii**. Finally, through intramolecular substitution of anion and the corresponding cyclic carbonate was produced along with the regeneration of catalyst for the next cycle. The synergistic effect of hydroxyl groups activating epoxide, imidazolium activating $CO_2$ and the lactate anion activating the nucleophilic attack of epoxide, which is helpful for the cycloaddition and improves the catalytic efficiency.

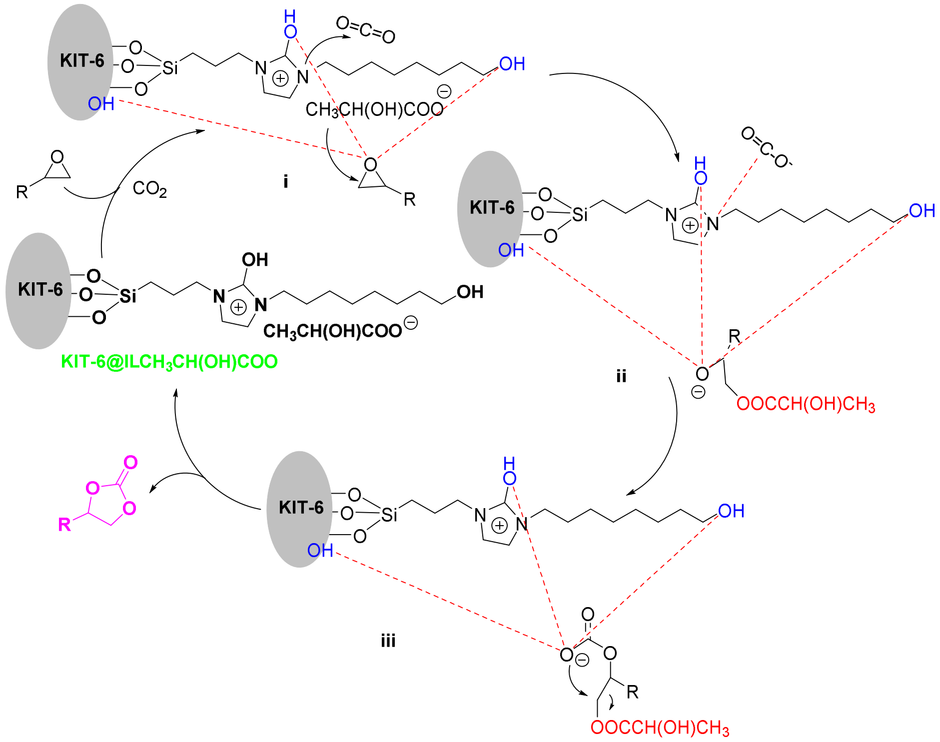

Scheme 3. Possible reaction mechanism for the cycloaddition of $CO_2$ with epoxides.

## CONCLUSIONS

In conclusion, a series of mesoporous KIT-6 supported lactate-functionalized basic ionic liquids KIT-6@IL$CH_3CH(OH)COO$ were prepared and tested as catalysts for the synthesis of cyclic carbonates by the cycloaddition of $CO_2$ with epoxides. The experiment demonstrated that the catalyst KIT-6@IL$CH_3CH(OH)COO$(0.6) possessing abundant active sites exhibited excellent activity in high to excellent yields (87%~99%) and selectivities (>99%), may be attributed to the synergetic effect between hydroxyl groups and lactate anion of ionic liquid. The catalyst having full utilization of active sites can be easily recovered and reused for six times without considerable reduction in catalytic activity. The protocol was found to be advantageous in terms of high to excellent yields, ease of isolation and reusability of the catalyst. This study confirmed that the the construction of synergistic catalytic active sites of mesoporous material supported ILs was a cost effective way that not only markedly enhanced the catalytic activity but also facilitated the operation and transport, which offered a broad application prospect in the practical application of green and high efficient catalytic process for the chemical fixation of carbon dioxide.

## ACKNOWLEDGEMENTS

This work was financially supported by the Research Foundation of Yichang Science and Technology Bureau (A21-3-009), Research Foundation of Hubei Three Gorges Laboratory (SC213010), 111 Project (D20015) and analysis and testing center of China Three Gorges University.

## REFERENCES

1. Markewitz, P.; Kuckshinrichs, W.; Leitner, W.; Linssen, J.; Zapp, P.; Bongartz, R.; Schreiber, A.; Müller, T.E. Worldwide innovations in the development of carbon capture technologies and the utilization of $CO_2$. *Energy Environ. Sci.* **2012**, 5, 7281-7305.
2. North, M.; Styring, P. Perspectives and visions on $CO_2$ capture and utilisation. *Faraday Discuss.* **2015**, 183, 489-502.
3. Ostovari, H.; Sternberg, A.; Bardow, A. Rock 'n' use of $CO_2$: Carbon footprint of carbon capture and utilization by mineralization. *Sustain. Energy Fuels* **2020**, 4, 4482-4496.
4. Kamphuis, A.J.; Picchioni, F.; Pescarmona, P.P. $CO_2$-fixation into cyclic and polymeric carbonates: principles and applications. *Green Chem.* **2019**, 21, 406-448.
5. Shaikh, R.R.; Pornpraprom, S.; D'Elia, V. Catalytic strategies for the cycloaddition of pure, diluted, and waste $CO_2$ to epoxides under ambient conditions. *ACS Catal.* **2018**, 8, 419-450.
6. Subramanian, S.; Song, Y.; Kim, D.; Yavuz, C.T. Redox and nonredox $CO_2$ utilization: Dry reforming of methane and catalytic cyclic carbonate formation. *ACS Energy Lett.* **2020**, 5, 1689-1700.
7. Prasad, D.; Patil, K.N.; Bhanushali, J.T.; Nagaraja, B.M.; Jadhav, A.H. Sustainable fixation of $CO_2$ into epoxides to form cyclic carbonates using hollow marigold $CuCo_2O_4$ spinel microspheres as a robust catalyst. *Catal. Sci. Technol.* **2019**, 9, 4393-4412.
8. Guo, L.; Lamb, K.J.; North, M. Recent developments in organocatalysed transformations of epoxides and carbon dioxide into cyclic carbonates. *Green Chem.* **2021**, 23, 77-118.
9. Chen, Z.; Yang, J. L.; Lu, X.Y.; Hu, L.F.; Cao, X.H.; Wu, G.P.; Zhang, X.H. Triethyl borane-regulated selective production of polycarbonates and cyclic carbonates for the coupling reaction of $CO_2$ with epoxides. *Polym. Chem.* **2019**, 10, 3621-3628.
10. Takaishi, K.; Okuyama, T.; Kadosaki, S.; Uchiyama, M.; Ema, T. Hemisquaramide tweezers as organocatalysts: Synthesis of cyclic carbonates from epoxides and $CO_2$. *Org. Lett.* **2019**, 21, 1397-1401.
11. Yepes, Y.R. Quintero, C.; Meléndez, D.O.; Daniliuc, C.G.; Martínez, J.; Rojas, R.S. Cyclic carbonates from $CO_2$ and epoxides catalyzed by tetra- and pentacoordinate amidinate aluminum complexes. *Organometallics* **2019**, 38, 469-478.
12. Sobrino, S.; Navarro, M.; Fernández-Baeza, J.; Sánchez-Barba, L.F.; Garcés, A.; Lara-Sánchez, A.; Castro-Osma, J.A. Efficient $CO_2$ fixation into cyclic carbonates catalyzed by NNO-scorpionate zinc complexes. *Dalton Trans.* **2019**, 48, 10733-10742.
13. Das, R.; Dhankhar, S.S.; Nagaraja, C.M. Construction of a bifunctional Zn(II)–organic framework containing a basic amine functionality for selective capture and room temperature fixation of $CO_2$. *Inorg. Chem. Front.* **2020**, 7, 72-81.
14. Bui, T.Q.; Konwar, L.J.; Samikannu, A.; Nikjoo, D.; Mikkola, J.P. Mesoporous melamine-formaldehyde resins as efficient heterogeneous catalysts for continuous synthesis of cyclic carbonates from epoxides and gaseous $CO_2$. *ACS Sustain. Chem. Eng.* **2020**, 8, 12852-12869.
15. Guo, F.; Zhang, X. Metal-organic frameworks for the energy-related conversion of $CO_2$ into cyclic carbonates. *Dalton Trans.* **2020**, 49, 9935-9947.
16. Dhankhar, S.S.; Nagaraja, C.M. Construction of a 3D porous Co(II) metal-organic framework (MOF) with Lewis acidic metal sites exhibiting selective $CO_2$ capture and conversion under mild conditions. *New J. Chem.* **2019**, 43, 2163-2170.

17. Pala, T.K.; Deb, D.; Bharadwaj, P.K. Metal-organic frameworks for the chemical fixation of $CO_2$ into cyclic carbonates. *Coordin. Chem. Rev.* **2020**, 408, 213173.
18. Prajapati, P.K.; Kumar, A.; Jain, S.L. First photocatalytic synthesis of cyclic carbonates from $CO_2$ and epoxides using CoPc/$TiO_2$ hybrid under mild conditions. *ACS Sustain. Chem. Eng.* **2018**, 6, 7799-7809.
19. Vagnoni, M.; Samorì, C.; Galletti, P. Choline-based eutectic mixtures as catalysts for effective synthesis of cyclic carbonates from epoxides and $CO_2$. *J. $CO_2$ Util.* **2020**, 42, 101302.
20. Comerford, J.W.; Ingram, I.D.V.; North, M.; Wu, X. Sustainable metal-based catalysts for the synthesis of cyclic carbonates containing five-membered rings. *Green Chem.* **2015**, 17, 1966-1987.
21. Alassmy, Y.A.; Pour, Z.A.; Pescarmona, P.P. Efficient and easily reusable metal-free heterogeneous catalyst beads for the conversion of $CO_2$ into cyclic carbonates in the presence of water as hydrogen-bond donor. *ACS Sustain. Chem. Eng.* **2020**, 8, 7993-8003.
22. Maeda, C.; Mitsuzane, M.; Ema, T. Chiral bifunctional metalloporphyrin catalysts for kinetic resolution of epoxides with carbon dioxide. *Org. Lett.* **2019**, 21, 1853-1856.
23. Subramanian, S.; Park, J.; Byun, J.; Jung, Y.; Yavuz, C.T. Highly efficient catalytic cyclic carbonate formation by pyridyl salicylimines. *ACS Appl. Mater. Inter.* **2018**, 10, 9478-9484.
24. Martínez, J.; Castro-Osma, J.A.; Earlam, A.; Alonso-Moreno, C.; Otero, A.; Lara-Sanchez, A.; North, M.; Rodríguez-Diéguez, A. Synthesis of cyclic carbonates catalysed by aluminium heteroscorpionate complexes. *Chem. Eur. J.* **2015**, 21, 9850- 9862.
25. Meléndez, D.O.; Lara-Sánchez, A.; Martínez, J.; Wu, X.; Otero, A.; Castro-Osma, J.A.; North, M.; Rojas, R.S. Amidinate aluminium complexes as catalysts for carbon dioxide fixation into cyclic carbonates. *ChemCatChem* **2018**, 10, 2271-2277.
26. Martínez, J.; Fernández-Baeza, J.; Sánchez-Barba, L.F.; Castro-Osma, J.A.; Lara-Sánchez, A.; Otero, A. An efficient and versatile lanthanum heteroscorpionate catalyst for carbon dioxide fixation into cyclic carbonates. *ChemSusChem* **2017**, 10, 2886-2890.
27. Amarasekara, A.S. Acidic ionic liquids. *Chem. Rev.* **2016**, 116, 6133-6183.
28. Aldroubi, S.; Brun, N.; Malham, I.B.; Mehdi, A. When graphene meets ionic liquids: a good match for the design of functional materials. *Nanoscale* **2021**, 13, 2750-2779.
29. Jin, Y.; Fang, S.; Chai, M.; Yang, L.; Hirano, S. Ether-functionalized trialkylimidazolium ionic liquids: Synthesis, characterization, and properties. *Ind. Eng. Chem. Res.* **2012**, 51, 11011-11020.
30. Sadeghi-Takallo, S.; Zare, A. Novel ionic liquid [$Et_3N$-$SO_3H$][$MeSO_3$]: Synthesis, characterization and catalytic performance for the synthesis of 14-aryl-14H-dibenzo[a,j]xanthenes. *Bull. Chem. Soc. Ethiop.* **2019**, 33, 69-76.
31. Nikpassand, M.; Fekri, L.Z.; Sahrapeima, S. Grinding technique for the tandem synthesis of bis coumarinyl methanes using [BDBDMIm]Br-CAN. *Bull. Chem. Soc. Ethiop.* **2017**, 31, 323-329.
32. Mohammadi, M.K.; Saghanezhad, S.J.; Razzaghi-asl, N. Dabco containing acidic poly(ionic liquid): An efficient catalyst for the one-pot Preparation of 2,3-dihydroquinazoline-4(1H)-ones. *Bull. Chem. Soc. Ethiop.* **2017**, 31, 535-544.
33. Wang, P.; Xu, Y.; Lin, Q.; Lu, M. Recent advances in the syntheses and properties of polynitrogen pentazolate anion *cyclo*-$N_5^-$ and its derivatives. *Chem. Soc. Rev.* **2018**, 47, 7522-7538.
34. Xu, Y.; Tian, L.; Li, D.; Wang, P.; Lu, M.A series of energetic *cyclo*-pentazolate salts: Rapid synthesis, characterization, and promising performance. *J. Mater. Chem. A* **2019**, 7, 12468-12479.
35. Xu, Y.; Wang, Q.; Shen, C.; Lin, Q.; Wang, P.; Lu, M. A series of energetic metal pentazolate hydrates. *Nature* **2017**, 549, 78-81.
36. Wang, P.C.; Xu, Y.G.; Wang, Q.; Shao, Y.L.; Lin, Q.H.; Lu, M. Self-assembled energetic coordination polymers based on multidentate pentazole *cyclo*-$N_5^-$. *Sci. China Mater.* **2019**, 62, 122-129.

37. Xu, Y.; Wang, P.; Lin, Q.; Du, Y.; Lu, M. Cationic and anionic energetic materials based on a new amphotère. *Sci. China Mater.* **2019**, 62, 751-758.
38. Goodrich, P.; Gunaratne, H.Q.N.; Jacquemin, J.; Jin, L.; Lei, Y.; Seddon, K.R. Sustainable cyclic carbonate production, utilizing carbon dioxide and azolate ionic liquids. *ACS Sustain. Chem. Eng.* **2017**, 5, 5635-5641.
39. Toda, Y.; Komiyama, Y.; Kikuchi, A.; Suga, H. Tetraarylphosphonium salt-catalyzed carbon dioxide fixation at atmospheric pressure for the synthesis of cyclic carbonates. *ACS Catal.* **2016**, 6, 6906-6910.
40. Hu, Y.; Zhang, R.L.; Fang, D. Quaternary phosphonium cationic ionic liquid/porous metal-organic framework as an efficient catalytic system for cycloaddition of carbon dioxide into cyclic carbonates. *Environ. Chem. Lett.* **2019**, 17, 501-508.
41. Liu, F.; Gu, Y.; Zhao, P.; Gao, J.; Liu, M. Cooperative conversion of $CO_2$ to cyclic carbonates in dual-ionic ammonium salts catalytic medium at ambient temperature. *ACS Sustain. Chem. Eng.* **2019**, 7, 5940-5945.
42. Liu, J.; Yang, G.; Liu, Y.; Zhang, D.; Hu, X.; Zhang, Z. Efficient conversion of $CO_2$ into cyclic carbonates at room temperature catalyzed by Al-salen and imidazolium hydrogen carbonate ionic liquids. *Green Chem.* **2020**, 22, 4509-4515.
43. Xin, B.; Hao, J. Imidazolium-based ionic liquids grafted on solid surfaces. *Chem. Soc. Rev.* **2014**, 43, 7171-7187.
44. Bordet, A.; Moos, G.; Welsh, C.; Licence, P.; Luska, K.L.; Leitner, W. Molecular control of the catalytic properties of rhodium nanoparticles in supported ionic liquid phase (SILP) systems. *ACS Catal.* **2020**, 10, 13904-13912.
45. Lanaridi, O.; Sahoo, A.R.; Limbeck, A.; Naghdi, S.; Eder, D.; Eitenberger, E.; Csendes, Z.; Schnürch, M.; Bica-Schröder, K. Toward the recovery of platinum group metals from a spent automotive catalyst with supported ionic liquid phases. *ACS Sustain. Chem. Eng.* **2021**, 9, 375-386.
46. Isaad, J. Acidic ionic liquid supported on silica-coated magnetite nanoparticles as a green catalyst for one-pot diazotization–halogenation of the aromatic amines. *RSC Adv.* **2014**, 4, 49333-49341.
47. Mdoe, J.E.G.; Makene, J.S.M. Removal of lead(II) ions from aqueous solutions using cashew nut shell liquid-templated thiol-silica materials. *Bull. Chem. Soc. Ethiop*. **2014**, 28, 363-372.
48. Kleitz, F.; Bérubé, F.; Guillet-Nicolas, R.; Yang, C. M.; Thommes, M. Probing adsorption, pore condensation, and hysteresis behavior of pure fluids in three-dimensional cubic mesoporous KIT-6 silica. *J. Phys. Chem. C* **2010**, 114, 9344-9355.
49. Villarroel-Rocha, D.; Godoy, A.A.; Toncón-Leal, C.; Villarroel-Rocha, J.; Moreno, M.S.; Bernini, M.C.; Narda, G.E.; Sapag, K. Synthesis of micro-mesoporous CPO-27-Mg@KIT-6 composites and their test in $CO_2$ adsorption. *New J. Chem.* **2020**, 44, 10056-10065.
50. Zhu, H.; Ramanathan, A.; Wu, J.F.; Subramaniam, B. Genesis of strong brønsted acid sites in WZr-KIT-6 catalysts and enhancement of ethanol dehydration activity. *ACS Catal.* **2018**, 8, 4848-4859.